

# Dalton Transactions

Accepted Manuscript



This is an *Accepted Manuscript*, which has been through the Royal Society of Chemistry peer review process and has been accepted for publication.

*Accepted Manuscripts* are published online shortly after acceptance, before technical editing, formatting and proof reading. Using this free service, authors can make their results available to the community, in citable form, before we publish the edited article. We will replace this *Accepted Manuscript* with the edited and formatted *Advance Article* as soon as it is available.

You can find more information about *Accepted Manuscripts* in the [Information for Authors](#).

Please note that technical editing may introduce minor changes to the text and/or graphics, which may alter content. The journal's standard [Terms & Conditions](#) and the [Ethical guidelines](#) still apply. In no event shall the Royal Society of Chemistry be held responsible for any errors or omissions in this *Accepted Manuscript* or any consequences arising from the use of any information it contains.

Cite this: DOI: 10.1039/c0xx00000x

www.rsc.org/xxxxxx

ARTICLE TYPE

# Breaking aggregation in a tetrathiafulvalene-fused zinc porphyrin by metal-ligand coordination to form a donor-acceptor hybrid for ultrafast charge separation and charge stabilization<sup>†</sup>

Atanu Jana,<sup>a</sup> Habtom B. Gobeze,<sup>b</sup> Masatoshi Ishida,<sup>c</sup> Toshiyuki Mori,<sup>d</sup> Katsuhiko Ariga,<sup>ae</sup> Jonathan P. Hill<sup>\*ae</sup> and Francis D'Souza<sup>\*b</sup>

Received (in XXX, XXX) Xth XXXXXXXXXX 20XX, Accepted Xth XXXXXXXXXX 20XX

DOI: 10.1039/b000000x

A novel electron rich, tetrathiafulvalene fused zinc porphyrin, (TTF)<sub>4</sub>PZn, has been newly synthesized and characterized using 10 spectral and electrochemical methods. In spite of the presence of the eight *t*-butyl groups, (TTF)<sub>4</sub>PZn exhibited appreciable aggregation in solution. Scanning electron microscopic (SEM) imaging of the aggregates revealed spherical particulate morphology. Attenuation of intermolecular aggregation was possible by metal-ligand coordination of a nitrogenous ligand. Further, using this strategy, donor-acceptor hybrid was formed by coordinating imidazole functionalized fullerene as an electron 15 and transient absorption spectroscopic techniques. The determined rate of charge separation,  $k_{CS}$  and rate of charge recombination,  $k_{CR}$  were found to be  $1.4 \times 10^{11} \text{ s}^{-1}$  and  $2.5 \times 10^6 \text{ s}^{-1}$ , respectively. The lower  $k_{CR}$  value indicate charge stabilization in the assembled donor-acceptor conjugate via an electron transfer – hole transfer mechanism.

## 1. Introduction

Aggregation of natural pigments such as chlorophylls and their 20 synthetic analogues, porphyrins and phthalocyanines is a very well-known phenomenon.<sup>1-3</sup> Molecular structures of the pigments often control the aggregation phenomenon either by  $\pi$ - $\pi$  interactions, metal ion- $\pi$  interactions, axial-ligand promoted interactions or macrocycle side chain binding with other units.<sup>4</sup> 25 Aggregates due to  $\pi$ - $\pi$  interactions can be categorised into H- or J-type, which respectively exhibit either blue- or red-shifted absorption bands accompanied by spectral broadening.<sup>5-6</sup> There is widespread interest in studying molecular aggregation due to their spectral properties, and possible technological applications 30 of these materials whose properties vary from those of the respective molecules and their crystalline forms. However, aggregation often results in reduced fluorescence quantum yields and lifetimes of photosensitizers, a disadvantage that restricts their applications in the study of photoinduced energy and 35 electron transfer relevant to light energy harvesting and solar fuel production.<sup>3</sup>

Over the past decade, significant attempts have been made to prepare  $\pi$ -extended or annulated oligopyrrolic compounds analogous to porphyrins that would possess better electron donor 40 properties. In one case, this was done by annulations of tetrathiafulvalenes (TTFs) at the  $\beta$ -positions of porphyrin making the resulting molecules extraordinarily electron rich. Hybrid TTF-annulated porphyrins<sup>7-13</sup> are particularly attractive because they contain both redox active sites and a chromophoric unit contained 45 within a single molecular framework.<sup>14-19</sup>

In the present study, we report the synthesis of a novel  $\pi$ -extended zinc porphyrin bearing four TTF substituents at its  $\beta$ -positions with 3,5-di-*t*-butyl-4-hydroxyphenyl groups at *meso*- 50 positions (Fig. 1). Due to the combination of these peripheral substituents, the porphyrin macrocycle is expected to reveal greater intrinsic electron donor character. This molecule, in spite of having eight *t*-butyl groups on the *meso*-aryl substituents, exhibited considerable aggregation in solution that compromised 55 the fluorescence emission. As demonstrated here, such aggregation could easily be attenuated by axial coordination of a nitrogenous ligand to recover the fluorescence. Furthermore, this strategy has been exploited to build a donor-acceptor hybrid by coordinating the well-known electron acceptor, fullerene 60 (functionalized with a phenylimidazole ligand).<sup>20-23</sup> Using femtosecond and nanosecond transient spectroscopic techniques, charge separation in the donor-acceptor hybrid was successfully demonstrated.

Insert Fig. 1 here

65 **Fig. 1.** Chemical structure of TTF fused ZnP, (TTF)<sub>4</sub>PZn, phenyl imidazole, PhIm, and the imidazole ligand bearing fullerene derivative C<sub>60</sub>Im used in the present study.

## 2. Experimental

### 2.2.1 Chemicals

3,5-Di-*t*-butyl-4-hydroxybenzaldehyde and propionic acid were purchased from Tokyo Kasei Chemical Co. and used as received without further purification. All other chemicals and

solvents used for synthesis were obtained from Tokyo Kasei Chemical Co., Wako Chemical Co., Fischer Chemical Co. or Aldrich Chemical Co. in reagent grade purity and used without further purification unless otherwise noted. TTF-pyrrole was prepared according to previously published procedures.<sup>24-25</sup> Analytical thin-layer chromatography (TLC) was performed on Merck silica gel 60 pre-coated on aluminium plates. Column chromatography was carried out using silica gel 60 (200 mesh, Merck). Preparative HPLC (GPC) analyses were performed on a JAI LC-908 instrument using a JAIJEL-1H and -2H columns. Tetra-*n*-butylammonium perchlorate, (*n*-Bu<sub>4</sub>N)ClO<sub>4</sub> used in electrochemical studies was from Fluka Chemicals. C<sub>60</sub>Im was synthesized according to our published method.<sup>26</sup>

### 2.2.2 Analyses

<sup>1</sup>H-NMR (300 MHz) and <sup>13</sup>C-NMR (75 MHz) spectra were recorded on a JEOL JNM-AL300 spectrometer. Chemical shifts ( $\delta$ -scale) are reported in ppm relative to residual solvent and internal standard signals (CDCl<sub>3</sub>: 7.29 ppm). MALDI-TOF mass spectra were recorded on a Kratos Axima-CFR-plus spectrometer using a DCTB, (*trans*-2-[3-(4-*tert*-butyl-phenyl)-2-methyl-2-propenyldene]malonitrile) as a matrix. UV-vis-NIR spectra were recorded on a Shimadzu UV-3600 spectrophotometer in dry CH<sub>2</sub>Cl<sub>2</sub> and 1,2-dichlorobenzene (DCB) solvents at 298 K. Other UV-visible spectral measurements were carried out either on a Shimadzu Model 2550 double monochromator UV-visible spectrophotometer or a Jasco V-670 spectrophotometer. Steady-state fluorescence spectra were measured by using a Horiba Jobin Yvon Nanolog UV-visible-NIR spectrofluorometer equipped with a PMT (for UV-visible) and InGaAs (for NIR) detectors. A right angle detection method was used for emission measurements. Differential pulse voltammograms were recorded on an EG&G 263A potentiostat/galvanostat using a three electrode system. A platinum button electrode was used as the working electrode. A platinum wire was used as the counter electrode and an Ag/AgCl electrode was used as the reference electrode. All solutions were purged using dry argon gas prior to electrochemical and spectral measurements. Scanning electron microscopy was carried out using a Hitachi S-4800 FE-SEM at an accelerating voltage of 5 kV on samples cast onto silicon substrates. Prior to observation, samples were coated with platinum (5 nm approx.) using a Hitachi S-1050 vacuum coater.

### 2.2.3 Laser flash photolysis

Samples were excited using a Panther OPO pumped by Nd:YAG laser (Continuum, SLII-10, 4-6 ns fwhm) with the powers of 1.5 or 3.0 mJ *per* pulse. Transient absorption measurements were performed using a continuous xenon lamp (150 W) and an InGaAs-PIN photodiode (Hamamatsu 2949) as probe light and detector, respectively. The output from the photodiodes and a photomultiplier tube was recorded with a digitizing oscilloscope (Tektronix, TDS3032, 300 MHz).

Femtosecond transient absorption spectroscopy experiments were conducted using an ultrafast source: Integra-C (Quantronix Corp.), an optical parametric amplifier: TOPAS (Light Conversion Ltd.) and a commercially available optical detection system: Helios provided by Ultrafast Systems LLC. The source for the pump and probe pulses were derived from the fundamental output of Integra-C (780 nm, 2  $\mu$ J/pulse and fwhm = 130 fs) at a repetition rate of 1 kHz. 75% of the fundamental output of the laser was introduced into TOPAS which has optical

frequency mixers resulting in tunable range from 285 nm to 1660 nm, while the rest of the output was used for white light generation. Typically, 2500 excitation pulses were averaged for 5 seconds to obtain the transient spectrum at a set delay time. Kinetic traces at appropriate wavelengths were assembled from the time-resolved spectral data. All measurements were conducted at 295 K.

### 2.2.4 DFT Calculations

Quantum mechanical calculations were performed using the Gaussian 09 program suite.<sup>27</sup> All calculations were carried out using the density functional theory (DFT) method with Becke's three-parameter hybrid exchange functional and the Lee-Yang-Parr correlation functional (B3LYP)<sup>28-29</sup> a basis set of 3-21G\* was employed for all atoms. Peripheral propyl groups were replaced with methyl groups to reduce the computational cost.

## 2.2 Synthesis

The target compound, (TTF)<sub>4</sub>PZn was synthesized according to Adler et al<sup>30</sup> by condensation of TTF-fused pyrrole with 3,5-di-*t*-butyl-4-hydroxybenzaldehyde with subsequent insertion of Zn<sup>2+</sup> by using the acetate method. As outlined in Scheme 1, the  $\beta$ -annulated TTF-porphyrins, (TTF)<sub>4</sub>PH<sub>2</sub> and its corresponding Zn(II)-complex was synthesized from the known TTF-annulated pyrrole (PrS-TTF-pyrrole) and 3,5-di-*t*-butyl-4-hydroxy benzaldehyde following Adler's method by a conventional pyrrole-aldehyde condensation reaction in refluxing propionic acid. The crude porphyrin was then subjected to several rounds of silica gel chromatographic separation. The products, isolated as different fractions were further subjected to recycling preparative HPLC-GPC (gel-permeation chromatography) to effect final purification.

The Zn(II)-complex of the isolated free-base TTF-porphyrin, (TTF)<sub>4</sub>PZn was then obtained by treating the free base form with Zn(OAc)<sub>2</sub>•2H<sub>2</sub>O in CHCl<sub>3</sub>/MeOH (10:1, v/v) and heating at reflux for 1 hour. Column chromatography over silica gel, followed by final GPC separation, gave the purified metalloporphyrin in good yields. All the compounds were well characterized by NMR, MALDI-TOF and HPLC-GPC. Freshly prepared and recrystallized samples were used for the photophysical and electrochemical studies.

**Insert Scheme 1 here (expand to two columns please)**

**Scheme 1:** Synthetic route for the TTF-porphyrins.

### 2.2.1 Synthesis of (TTF)<sub>4</sub>PH<sub>2</sub>

Typically, in a 250 mL two-necked RB flask, PrS-TTF-pyrrole (0.392 g, 1 mmol) and 3,5-di-*t*-butyl-4-hydroxybenzaldehyde (0.234 g, 1 mmol) were dried overnight under reduced pressure. Propionic acid (30 mL) was added and the resulting mixture was refluxed for 3 hours. Propionic acid was evaporated under reduced pressure and the resulting solid mass was washed with dry methanol yielding a dark solid which was then dissolved in dichloromethane and passed through a short alumina column to remove polymeric and other polar impurities. The target porphyrin was isolated by flash column chromatography on silica gel eluting with 1:1 dichloromethane/hexane mixture. Further purification was by gel permeation chromatography (GPC) using JAI LC-908 with CHCl<sub>3</sub> as eluent. Finally, the product was recrystallized from CHCl<sub>3</sub> and hexane and used for

characterization and other experiments. Yield ~20%;  $^1\text{H}$  NMR (300 MHz,  $\text{CDCl}_3$ , 298 K, TMS):  $\delta$  = -2.96 (bs, 2H), 1.01 (t,  $J$  = 7.2 Hz, 24H), 1.64-1.69 (m, 88H), 2.77 (t,  $J$  = 7.5 Hz, 16H), 5.79 (s, 4H), 7.73 (s, 8H),  $^{13}\text{C}$ -NMR spectrum (75 MHz,  $\text{CDCl}_3$ , 298 K, TMS): 13.2, 23.1, 30.3, 34.8, 38.3, 118.1, 127.4, 129.4, 129.8, 136.7, 146.5, 154.6, 156.0; MALDI-TOF-MS:  $m/z$  calcd for  $\text{C}_{116}\text{H}_{142}\text{N}_4\text{O}_4\text{S}_{24}$ : 2425.953; found: 2425.3; elemental analysis calcd (%) for  $\text{C}_{116}\text{H}_{142}\text{N}_4\text{O}_4\text{S}_{24}$ : C 57.43, H 5.90, N 2.31, S 31.72; found: C 57.41, H 5.84, N 2.36, S 31.79.

### 2.2.2 Synthesis of $(\text{TTF})_4\text{PZn}$

Complexation with Zn(II) was achieved by subjecting the free base  $(\text{TTF})_4\text{PH}_2$  (0.06 gm, 0.025 mmol) to treatment with  $\text{Zn}(\text{OAc})_2 \cdot 2\text{H}_2\text{O}$  (0.055 gm, 0.25 mmol) in  $\text{CHCl}_3$ :MeOH (10:1) at reflux for 1 hour under Ar. After partitioning of the reaction mixture between chloroform and water, the chloroform layer was dried over anhydrous  $\text{MgSO}_4$ . After filtration and evaporation of solvents, purification was by gel permeation chromatography (GPC) using JAI LC-908 with  $\text{CHCl}_3$  as eluent (typically involving three purification cycles). The product was isolated in nearly quantitative yield. The final product was recrystallized from  $\text{CHCl}_3$ -hexane mixture.  $^1\text{H}$  NMR (300 MHz,  $\text{CDCl}_3$ , 298 K, TMS):  $\delta$  = 1.00 (t,  $J$  = 7.2 Hz, 24H), 1.61-1.68 (m, 88H), 2.76 (t,  $J$  = 7.2 Hz, 16H), 5.76 (s, 4H), 7.71 (s, 8H);  $^{13}\text{C}$  NMR spectrum (75 MHz,  $\text{CDCl}_3$ , 298 K, TMS):  $\delta$  = 13.2, 23.1, 30.3, 34.8, 38.3, 119.0, 124.7, 127.4, 129.4, 130.4, 136.7, 141.1, 142.0, 155.9, 166.3; MALDI-TOF-MS:  $m/z$  calcd for  $\text{C}_{116}\text{H}_{140}\text{N}_4\text{O}_4\text{S}_{24}\text{Zn}$ : 2489.33; found: 2490.77; elemental analysis calcd (%) for  $\text{C}_{116}\text{H}_{140}\text{N}_4\text{O}_4\text{S}_{24}\text{Zn}$ : C 55.97, H 5.67, N 2.25, S 30.91; found: C 55.93, H 5.59, N 2.30, S 30.85.

## 3. Results and discussion

### 3.1 Absorption and fluorescence studies

Fig. 2 shows the absorption spectrum of  $(\text{TTF})_4\text{PZn}$  at different concentrations in *o*-dichlorobenzene (DCB). The Soret band located at 448 nm has a shoulder at 464 nm, while the Q-band is broad covering the region 550-800 nm. The red-shifted absorption bands, as compared to that of pristine tetraphenylporphyrinatozinc(II) (PZn,  $\lambda_{\text{max}} = 422$  nm) can be attributed to the extended  $\pi$ -system of  $(\text{TTF})_4\text{PZn}$  and charge transfer type interactions between the PZn and fused TTF entities. However, the intensity ratio of the Soret and the shoulder bands varies with concentration suggesting aggregation. As predicted for aggregated systems,<sup>1-3</sup> a plot of absorbance vs. concentration (Fig. 2 inset), revealed non-linear behaviour. It should also be noted here that the aggregation behaviour of  $(\text{TTF})_4\text{PZn}$  appears to be dependent on solution history so that measurements were always made on freshly prepared solutions. Peak shifts, especially in the visible range were often observed.

#### Insert Fig. 2 here

Fig. 2. Absorption spectrum of  $(\text{TTF})_4\text{PZn}$  at different concentrations in DCB ( $5 \times 10^{-6}$  M –  $4 \times 10^{-4}$  M). Inset: Beer-Lambert plot showing non-linear trend ( $\lambda_{\text{monitored}} = 448$  nm).

Attempts were also made to understand the nature and morphology of aggregated species. As shown in Fig. 3, deposition from various solvents permits observation of nanometric spherical aggregates of 100-300 nm diameters. In addition, dilution of solutions of  $(\text{TTF})_4\text{PZn}$  unexpectedly lead to

emergence of a new red-shifted shoulder band at the Soret, which we tentatively assign as being due to *J*-aggregation (see Fig. 2 above).<sup>31-32</sup> Emergence of this band at high dilution is thought to be caused by intermolecular charge transfer interactions (due to TTF substituents) that favour aggregation. The form of the aggregates could not be observed by electron microscopy presumably due to their small size - deposition of solutions lead only to featureless films.

#### Insert Fig. 3 here

Fig. 3. SEM image of aggregates of  $(\text{TTF})_4\text{ZnP}$  revealing their spherical particulate morphology. Scale bars: 2  $\mu\text{m}$  (left); 500 nm (right). The lower image was obtained with the substrate tilted at an angle of 35 degrees from the beam normal axis. A single drop of solution of  $(\text{TTF})_4\text{ZnP}$  ( $\sim 10^{-4}$  M) in chloroform containing  $\sim 5\%$  methanol was allowed to evaporate on the substrate prior to drying in vacuo and coating with platinum ( $\sim 5$  nm).

We found that aggregation processes and uncertainties due to the resulting structures could be largely eliminated by coordinating a nitrogenous base at the zinc(II) centre. For this, first,  $(\text{TTF})_4\text{PZn}$  was treated with phenylimidazole, PhIm in a noncoordinating solvent such as DCB. As shown in Fig. 4a, addition of PhIm resulted in a spectrum that resembled that of a monomeric zinc porphyrin. That is, the broad shoulder band to the Soret band located in the 495 nm range and the broad band located in the 715 nm range diminished in intensity with concomitant increase of zinc porphyrin Soret at 454 nm and a visible band at 575 nm. Isosbestic points at 420 and 594 nm were observed indicating existence of a single equilibrium. The final spectrum resembles that of the monomeric zinc porphyrin in dilute chloroform.<sup>26</sup> This suggests that formation of  $(\text{TTF})_4\text{PZn}$ :PhIm complex disperses aggregates of  $(\text{TTF})_4\text{PZn}$  ostensibly by obstructing intermolecular stacking interactions. Furthermore, the binding constant, *K* for the complex formation process was calculated by constructing a Benesi-Hildebrand plot<sup>33</sup> as shown in Fig. 4a inset. The *K* value for this process was found to be  $1.3 \pm 0.13 \times 10^6 \text{ M}^{-1}$  which was about two orders of magnitude greater than that reported for the same ligand binding to PZn.<sup>26</sup>

#### Inset Fig. 4 here

Fig. 4. (a) Effect of added PhIm on (a) absorption and (b) fluorescence spectrum of  $(\text{TTF})_4\text{PZn}$ . The sample was excited at the Soret band maxima. The inset in (a) shows Benesi-Hildebrand plot constructed to evaluate the binding constant.

As mentioned earlier, aggregation generally diminishes fluorescence intensity of organic sensitizers.<sup>1-3</sup> This seems to be also the case with the present  $(\text{TTF})_4\text{PZn}$  compound wherein both aggregation and intramolecular charge transfer between porphyrin  $\pi$ -system with TTF units diminish fluorescence. As shown in Fig. 4b, the fluorescence spectrum of  $(\text{TTF})_4\text{PZn}$  revealed two bands located at 610 and 668 nm. These bands are slightly red-shifted compared to pristine ZnP as a consequence of extended  $\pi$ -conjugation as a consequence of four TTF entities. Addition of PhIm increased the fluorescence and at the saturation point, this increase was about 43%. However, the final fluorescence intensity of  $(\text{TTF})_4\text{PZn}$ :PhIm was weaker than that of pristine ZnP bound to ImPh (<40%) since the fused TTF moieties of  $(\text{TTF})_4\text{PZn}$  promote intramolecular charge transfer thus diminishing the overall fluorescence.

Binding of C<sub>60</sub>Im to (TTF)<sub>4</sub>PZn followed a spectral trend similar to that of ImPh binding (Fig. 5). The broad Soret and visible bands became narrower with a concurrent increase in intensity. The final complex, (TTF)<sub>4</sub>Zn:C<sub>60</sub>Im, had the Soret band at 460 nm and visible band at 583 nm (Fig. 5a). Binding constant *K* determined from the Benesi-Hildebrand plot was found to be  $2.1 \pm 0.12 \times 10^5 \text{ M}^{-1}$  (Fig. 5a inset), an order of magnitude greater than that reported for C<sub>60</sub>Im binding to pristine ZnP.<sup>26</sup> Interestingly, C<sub>60</sub>Im binding also causes fluorescence quenching (Fig. 3b) in contrast to that observed for ImPh binding where an increase in fluorescence was observed. This suggests that the coordinated fullerene electron acceptor might be involved in light-induced electron transfer.

Insert Fig. 5 here

Fig. 5. (a) Effect of added ImC<sub>60</sub> on (a) absorption and (b) fluorescence spectra of (TTF)<sub>4</sub>PZn in DCB. The sample was excited at the Soret band maximum. The inset in (a) shows the Benesi-Hildebrand plot constructed to evaluate the binding constant.

### 3.2 Electrochemistry and computational studies

To determine the redox potentials of (TTF)<sub>4</sub>PZn and the (TTF)<sub>4</sub>PZn:C<sub>60</sub>Im complex, differential pulse voltammetry (DPV) experiments were performed in DCB containing 0.1 M (*n*-Bu<sub>4</sub>N)ClO<sub>4</sub>. On the cathodic side, (TTF)<sub>4</sub>PZn revealed two one-electron reductions located at -1.67 V and -1.95 V vs. Fc/Fc<sup>+</sup> involving the porphyrin macrocycle (Fig. 6a). On the anodic side, peaks corresponding to both TTF and PZn entities were observed. Four anodic processes at -0.06, 0.03, 0.35 and 0.41 V, each with peak currents twice that of the reduction peaks, were observed. By comparing the oxidation potential of these waves to that of pristine TTF, these processes have been ascribed to the formation of TTF<sup>•+</sup> and TTF<sup>2+</sup> of the (TTF)<sub>4</sub>PZn macrocycle. The splitting of the oxidation wave is indicative of interactions between the TTF moieties and the porphyrin  $\pi$ -system. At more positive potentials, two additional one-electron oxidation processes located at 0.97 and 1.38 V vs. Fc/Fc<sup>+</sup> were observed. These can be assigned to the formation of ZnP<sup>•+</sup> and ZnP<sup>2+</sup> species, respectively. The anodically shifting of peaks due to these processes compared to pristine ZnP (0.28 and 0.62 V vs. Fc/Fc<sup>+</sup>) indicates the relatively electron deficient nature of the porphyrin (against neutral (TTF)<sub>4</sub>PZn) due to the influence of four interacting TTF<sup>2+</sup> entities possessing a total of eight positive charges. It is important to note that although there is substantial interaction, the PZn and TTF entities of (TTF)<sub>4</sub>PZn retain their respective properties rather than behaving as a single molecule. The acceptor, C<sub>60</sub>Im undergoes three one-electron reductions at -1.12, -1.51 and -1.96 V vs. Fc/Fc<sup>+</sup>, respectively (Fig. 6b). Upon complexation of C<sub>60</sub>Im to (TTF)<sub>4</sub>PZn to form (TTF)<sub>4</sub>PZn:C<sub>60</sub>Im, no significant changes corresponding to either fullerene or TTF centred oxidations were observed, however, oxidation peaks corresponding to PZn underwent a small anodic shift of 20 mV.

Insert Fig. 6 here

Fig. 6. Differential pulse voltammogram (DPV) of (a) (TTF)<sub>4</sub>PZn and (b) C<sub>60</sub>Im in DCB containing 0.1 M (TBA)ClO<sub>4</sub>. Scan rate = 5 mV/s, pulse width = 0.25 s, pulse height = 0.025 V.

Computational studies at the B3LYP/3-21G\* level<sup>27</sup> were performed to visualize geometry and electronic structure of (TTF)<sub>4</sub>PZn and its C<sub>60</sub>Im complex. The calculated conformations

of the macrocyclic core planes for the free-base derivative and its Zn(II)-complex were found to be nearly planar, findings that are consistent with the literature data reported earlier.<sup>9-10</sup> The systems were analyzed in accord with the Goutemann four orbital model used to describe the electronic features of ordinary porphyrins. Using this analysis, the molecular orbitals (MOs) of the (TTF)<sub>4</sub>PZn and (TTF)<sub>4</sub>PZn:C<sub>60</sub>Im were characterized by electron density distributions expected for CT molecules. As shown in Fig. 7a and b, the HOMOs of (TTF)<sub>4</sub>PZn are mainly localized on the TTF entities with weak contributions from the porphyrin  $\pi$ -system, suggesting intramolecular interactions between TTF and PZn entities. However, the LUMOs were found to involve only the PZn  $\pi$ -system. These results agree well with the electrochemical results discussed earlier. The HOMO of the optimized (TTF)<sub>4</sub>PZn:C<sub>60</sub>Im complex is located mainly on the TTF entities with some contributions on the PZn while the LUMO is fully localized on the fullerene group (Fig. 7c and d). It is important to note that axial coordination of the fullerene imposed no steric constraints on the TTF entities of (TTF)<sub>4</sub>PZn.

Insert Fig. 7 here

Fig. 7. HOMO and LUMO contour surfaces of (TTF)<sub>4</sub>PZn (a and b) and (TTF)<sub>4</sub>PZn:C<sub>60</sub>Im (c and d).

By using the redox, optical and computational data, the free-energy change of charge separation,  $\Delta G_{CS}$  was estimated according to Weller's approach.<sup>34</sup> These calculations revealed that charge separation from the (TTF)<sub>4</sub>PZn\* ( $E_{0,0} = 2.03 \text{ eV}$ ) should be an exothermic process leading to production of the radical ion-pairs (TTF)<sub>4</sub>PZn<sup>•+</sup>:C<sub>60</sub>Im<sup>•-</sup> ( $\Delta G_{CS} = -0.16 \text{ eV}$ ) or ((TTF)<sub>3</sub>TTF<sup>•+</sup>)PZn:C<sub>60</sub>Im<sup>•-</sup> ( $\Delta G_{CS} = -1.05 \text{ eV}$ ). These results suggest that hole migration from the initial (TTF)<sub>4</sub>PZn<sup>•+</sup>:C<sub>60</sub>Im<sup>•-</sup> to produce ((TTF)<sub>3</sub>TTF<sup>•+</sup>)PZn:C<sub>60</sub>Im<sup>•-</sup> within the complex is a thermodynamically feasible process. This process is expected to generate long-lived charge separated states.<sup>35-44</sup>

### 3.3 Femtosecond and nanosecond transient absorption studies

In order to establish that charge separation occurs in (TTF)<sub>4</sub>PZn:C<sub>60</sub>Im, transient absorption studies were performed. First, (TTF)<sub>4</sub>PZn was chemically oxidized using nitrosonium hexafluoroborate to locate the absorption bands of [(TTF)<sub>4</sub>PZn]<sup>•+</sup>. As shown in Fig. S1 in the electronic supplemental section (ESI), this oxidation procedure revealed new absorption bands at 478, 580 and 641 nm. Singlet-singlet energy transfer from <sup>1</sup>PZn\* to C<sub>60</sub> was ruled out as one of the quenching mechanisms due to the lack of absorbance of C<sub>60</sub> in the wavelength region of PZn emission. Fig. S2 in ESI shows the femtosecond transient absorption spectrum of (TTF)<sub>4</sub>PZn (excited at 400 nm of 100 fs pulses) at the indicated time intervals. Immediately after excitation (< 1 ps), positive peaks at 512 and 866 nm and negative peaks at 467 and 590 nm were observed. The positive peaks are attributed to formation of the singlet excited state of (TTF)<sub>4</sub>PZn whereas the negative peaks are the inverse of the ground state absorption bands. New bands at 564, 662 and 727 nm gradually appeared with recovery of the ground state band at 467 nm. These spectral changes can be attributed to intramolecular charge transfer involving TTF and ZnP entities. The transient species decayed in less than 200 ps indicating a rapid charge recombination.

Fig. 8a shows transient absorption spectra for

(TTF)<sub>4</sub>PZn:C<sub>60</sub>Im at different time intervals. Features in the initially measured spectra are similar to those observed for (TTF)<sub>4</sub>PZn. However, over time new transient bands emerged at 1000 nm, corresponding to C<sub>60</sub><sup>•-</sup>, and in the 650-700 nm range, corresponding to ZnP<sup>•+</sup>.<sup>45</sup> Another new transient band at 570 nm due to the formation of TTF<sup>•+</sup> also emerged with concurrent decay of ZnP<sup>•+</sup> suggesting a competitive hole transfer process. Radical cation and radical anion bands were persistent beyond the 3 ns time window of the instrument (Fig. 8b). By monitoring the growth of C<sub>60</sub><sup>•-</sup>, the rate of charge separation, *k*<sub>CS</sub> was determined to be 1.4 × 10<sup>11</sup> s<sup>-1</sup>, indicating occurrence of ultrafast charge separation in this supramolecular donor-acceptor complex.

Insert Fig. 8 here

**Fig. 8.** (a) Femtosecond transient absorption spectra of (TTF)<sub>4</sub>PZn:C<sub>60</sub>Im complex at the indicated time intervals in DCB. (b) Time profile of the C<sub>60</sub><sup>•-</sup> peak monitored at 1000 nm.

In order to obtain a value for the rate of charge recombination, *k*<sub>CR</sub>, nanosecond transient measurements were performed. Fig. 9a shows the transient absorption spectrum at the indicated time intervals for the (TTF)<sub>4</sub>PZn:C<sub>60</sub>Im complex in DCB. Transient features in the visible and near-IR region, relevant to ((TTF)<sub>3</sub>TTF<sup>•+</sup>)ZnP:C<sub>60</sub>Im<sup>•-</sup> radical ion-pair were observed. To evaluate *k*<sub>CR</sub>, the decay of C<sub>60</sub><sup>•-</sup> at 1000 nm was monitored. As shown in Fig. 9b, the decay followed a biexponential process. A faster process with time constant of 0.03 μs and a slower process with time constant of 0.40 μs resulted in *k*<sub>CR</sub> values of 3.3 × 10<sup>7</sup> s<sup>-1</sup> and 2.5 × 10<sup>6</sup> s<sup>-1</sup>, respectively. These *k*<sub>CR</sub> values are lower than those reported for the PZn:C<sub>60</sub>Im complex (2.5 × 10<sup>8</sup> s<sup>-1</sup>).<sup>9</sup> These results support charge stabilization in the investigated supramolecular complex (TTF)<sub>4</sub>PZn:C<sub>60</sub>Im.

Insert Fig. 9 here

**Fig. 9.** (a) Nanosecond transient absorption spectra of the (TTF)<sub>4</sub>PZn:C<sub>60</sub>Im complex in N<sub>2</sub> saturated DCB at the indicated time intervals (λ<sub>ex</sub> = 355 nm of 6 ns laser pulse). (b) Time profile of the C<sub>60</sub><sup>•-</sup> peak at 1000 nm.

#### 4. Summary

In summary, tetrathiafulvalene fused zinc porphyrin as a charge stabilizing electron donor has been newly synthesized and characterized. Metal-ligand axial coordination has been effectively used to eliminate molecular aggregation observed in this large conjugated porphyrin π-system. This strategy is further utilized to form a novel donor-acceptor complex. (TTF)<sub>4</sub>PZn forms a stable complex with C<sub>60</sub>Im and the structure of the resulting (TTF)<sub>4</sub>PZn:C<sub>60</sub>Im complex was established using spectral, electrochemical and computational methods. Photoinduced electron transfer from the singlet excited porphyrin was established from transient absorption spectroscopic studies wherein charge stabilization as a result of an electron transfer followed by hole-transfer mechanism was demonstrated, signifying the importance of the present approach and that of donor-acceptor complexes in light energy harvesting applications.

This research was partly supported by the World Premier International Research Center Initiative on Materials Nanoarchitectonics from MEXT, Japan, and by the Core

Research for Evolutional Science and Technology (CREST) program of JST, Japan. FD acknowledges support from the NSF (Grant Nos. 1110942 and 1401188).

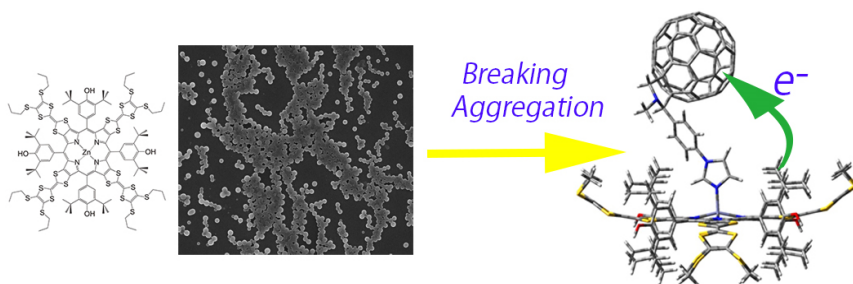
#### Notes and references

- <sup>60</sup> <sup>a</sup>Supermolecules Group, WPI center for Materials Nanoarchitectonics, National Institute for Materials Science (NIMS), Namiki 1-1, Tsukuba, Ibaraki 3050044, Japan. E-mail: jonathan.hill@nims.go.jp
- <sup>65</sup> <sup>b</sup>Department of Chemistry, University of North Texas, 1155 Union Circle, 305070, Denton, Texas 76203-5017, United States. E-mail: Francis.DSouza@UNT.edu
- <sup>70</sup> <sup>c</sup>Education Center for Global Leaders in Molecular Systems for Devices, Kyushu University, Fukuoka 819-0395, Japan.
- <sup>75</sup> <sup>d</sup>Fuel Cell Materials Group, National Institute for Materials Science (NIMS), Namiki 1-1, Tsukuba, Ibaraki 3050044, Japan.
- <sup>80</sup> <sup>e</sup>JST-CREST, Gobancho, Chiyoda-ku, Tokyo 102-0075, Japan
- <sup>85</sup> †Electronic Supplementary Information (ESI) available: HOMO and LUMO of (TTF)<sub>4</sub>PZn, spectral changes during chemical oxidation of (TTF)<sub>4</sub>PZn, and femtosecond transient absorption spectra of (TTF)<sub>4</sub>PZn. See DOI: 10.1039/b000000x/.
- <sup>90</sup> 1 W. I. White in *The Porphyrin* Ed. D. Dolphin, Academic Press, New York, Vol. 5, Chapter 7, 1978.
- <sup>95</sup> 2 D. C. Barber, R. A. Freitag and D. G. Whitten, *J. Phys. Chem.*, 1991, **95**, 4074.
- <sup>100</sup> 3 N. K. Maiti, S. Mazumdar and N. Periasamy, *J. Phys. Chem. B*, 1998, **102**, 1528.
- <sup>105</sup> 4 *Supramolecular Chemistry*, ed. J. W. Steed and J. L. Atwood, John Wiley and Sons, Chichester, 2009, 2<sup>nd</sup> edition.
- <sup>110</sup> 5 *H-aggregates*: A. J. Fleming, J. N. Coleman, A. B. Dalton, A. Fechtenkötter, M. D. Watson, K. Müllen, H. J. Byrne and W. J. Blau, *J. Phys. Chem. B*, 2003, **107**, 37.
- <sup>115</sup> 6 *J-aggregates*: F. Würthner, T. E. Kaiser and C. R. Saha-Möller, *Angew. Chem. Int. Ed.*, 2011, **50**, 3376.
- <sup>120</sup> 7 J. Becher, T. Brimert, J. O. Jeppesen, J. Z. Pedersen, R. Zubarev, T. Björnholm, N. Reitzel, T. R. Jensen, K. Kjaer and E. Levillain, *Angew. Chem. Int. Ed.*, 2001, **40**, 2497.
- <sup>125</sup> 8 H. Li, J. O. Jeppesen, E. Levillain and J. Becher, *Chem. Commun.*, 2003, 846.
- <sup>130</sup> 9 K. A. Nielsen, E. Levillain, V. M. Lynch, J. L. Sessler and J. O. Jeppesen, *Chem. Eur. J.*, 2009, **15**, 506.
- <sup>135</sup> 10 A. Jana, M. Ishida, K. Kwak, Y.-M. Sung, D. Kim and J. L. Sessler, *Chem. Eur. J.*, 2013, **19**, 338.
- <sup>140</sup> 11 S. Fukuzumi, K. Ohkubo, Y. Kawashima, D. S. Kim, J. S. Park, A. Jana, V. M. Lynch, D. Kim and J. L. Sessler, *J. Am. Chem. Soc.* 2011, **133**, 15938.
- <sup>145</sup> 12 H. Jia, B. Schmid, S.-X. Liu, M. Jaggi, P. Monbaron, S. V. Bhosale, S. Rivadehi, S. J. Langford, L. Sanguinet, E. Levillain, M. E. El-Khouly, Y. Morita, S. Fukuzumi and S. Decurtins, *ChemPhysChem* 2012, **13**, 3370.
- <sup>150</sup> 13 N. L. Bill, M. Ishida, S. Bähring, J. M. Lim, S. Lee, C. M. Davis, V. M. Lynch, K. A. Nielsen, J. O. Jeppesen, K. Ohkubo, S. Fukuzumi, D. Kim and J. L. Sessler, *J. Am. Chem. Soc.* 2013, **135**, 10852.
- <sup>155</sup> 14 K. N. Ferreira, T. M. Iverson, K. Maghlaoui, J. Barber and S. Iwata, *Science*, 2004, **303**, 1831.
- <sup>160</sup> 15 L. M. Utschig and M. C. Thurnauer, *Acc. Chem. Res.*, 2004, **37**, 439.
- <sup>165</sup> 16 B. Loll, J. Kern, W. Saenger, A. Zouni and J. Biesiadka, *Nature*, 2005, **438**, 1040.
- <sup>170</sup> 17 J. P. McEvoy and G. W. Brudvig, *Chem. Rev.*, 2006, **106**, 4455.
- <sup>175</sup> 18 C. F. Yocum, *Coord. Chem. Rev.*, 2007, **252**, 296.
- <sup>180</sup> 19 H. Imahori, N. V. Tkachenko, V. Vehmanen, K. Tamaki, H. Lemmetyinen, Y. Sakata and S. Fukuzumi, *J. Phys. Chem. A*, 2001, **105**, 1750.
- <sup>185</sup> 20 M. E. El-Khouly, O. Ito, P. M. Smith and F. D'Souza, *J. Photochem. Photobiol. C*, 2004, **5**, 79.
- <sup>190</sup> 21 F. D'Souza and O. Ito, *Chem. Soc. Rev.*, 2012, **41**, 86.
- <sup>195</sup> 22 F. D'Souza, A. S. D. Sandanayaka, and O. Ito in *Organic Nanomaterials* Eds. T. Torres and G. Bottari, Wiley-VCH, Weinheim, 2013, pp 187-204.

- 23 S. Fukuzumi and T. Kojima, *J. Mater. Chem.*, 2008, **18**, 1427.
- 24 C. Wang, A. S. Batsanov, M. R. Bryce, J. A. K. Howard, *Synthesis*, **1998**, 1615.
- 25 J. O. Jeppesen, K. Takimiya, F. Jensen, T. Brimert, K. Nielsen, N. Thorup, J. Becher, *J. Org. Chem.* **2000**, *65*, 5794.
- 26 F. D'Souza, G. R. Deviprasad, M. E. Zandler, V. T. Hoang, A. Klykov, M. VanStipdonk, A. Perera, M. E. El-Khouly, M. Fujitsuka and O. Ito, *J. Phys. Chem. A*, 2002, **106**, 3243.
- 27 Gaussian 09, Revision A.1, M. J. Frisch, G. W. Trucks, H. B. Schlegel, G. E. Scuseria, M. A. Robb, J. R. Cheeseman, G. Scalmani, V. Barone, B. Mennucci, G. A. Petersson, H. Nakatsuji, M. Caricato, X. Li, H. P. Hratchian, A. F. Izmaylov, J. Bloino, G. Zheng, J. L. Sonnenberg, M. Hada, M. Ehara, K. Toyota, R. Fukuda, J. Hasegawa, M. Ishida, T. Nakajima, Y. Honda, O. Kitao, H. Nakai, T. Vreven, J. A. Montgomery, Jr., J. E. Peralta, F. Ogliaro, M. Bearpark, J. J. Heyd, E. Brothers, K. N. Kudin, V. N. Staroverov, R. Kobayashi, J. Normand, K. Raghavachari, A. Rendell, J. C. Burant, S. S. Iyengar, J. Tomasi, M. Cossi, N. Rega, N. J. Millam, M. Klene, J. E. Knox, J. B. Cross, V. Bakken, C. Adamo, J. Jaramillo, R. Gomperts, R. E. Stratmann, O. Yazyev, A. J. Austin, R. Cammi, C. Pomelli, J. W. Ochterski, R. L. Martin, K. Morokuma, V. G. Zakrzewski, G. A. Voth, P. Salvador, J. J. Dannenberg, S. Dapprich, A. D. Daniels, Ö. Farkas, J. B. Foresman, J. V. Ortiz, J. Cioslowski, D. J. Fox, Gaussian, Inc., Wallingford CT, **2009**.
- 28 A. D. Becke, *J. Chem. Phys.* **1993**, *98*, 5648.
- 29 R.-P. Öscar, Y. Luo, H. Ågren, *J. Chem. Phys.* **2006**, *124*, 094 310-1.
- 30 A. D. Adler, F. R. Longo, J. D. Finarelli, J. Goldmacher, J. Assour and L. Korsakoff, *J. Org. Chem.*, 1967, **32**, 476.
- 31 E. E. Jelley, *Nature* 1936, **138**, 1009.
- 32 G. Scheibe *Angew. Chem.* 1937, **50**, 212.
- 33 H. A. Benesi and J. H. Hildebrand, *J. Am. Chem. Soc.*, 1949, **71**, 2703.
- 34 A. Weller, *Z. Phys. Chem.*, 1982, **132**, 93.
- 35 V. Sgobba and D. M. Guldi, *Chem. Soc. Rev.*, 2009, **38**, 165.
- 36 S. Fukuzumi, *Phys. Chem. Chem. Phys.*, 2008, **10**, 2283.
- 37 F. D'Souza and O. Ito, *Molecules*, 2012, **17**, 5816.
- 38 M.E. El-Khouly, S. Fukuzumi, F. D'Souza, *ChemPhysChem*, 2014, **15**, 30.
- 39 C. G. Claessens, D. González-Rodríguez and T. Torres, *Chem. Rev.* 2002, **102**, 835.
- 40 S. Fukuzumi, K. Ohkubo, F. D'Souza and J. L. Sessler, *Chem. Commun.* 2012, **48**, 9801.
- 41 H. Imahori, K. Tamaki, Y. Araki, Y. Sekiguchi, O. Ito, Y. Sakata, and S. Fukuzumi, *J. Am. Chem. Soc.*, 2002, **124**, 5165.
- 42 A. Satake and Y. Kobuke, *Org. Biomol. Chem.*, 2007, **5**, 1679.
- 43 D. I. Schuster, K. Li and D. M. Guldi, *C. R. Chimie*, 2006, **9**, 892.
- 44 C. A. Wijesinghe, M. E. El-Khouly, M. E. Zandler, S. Fukuzumi and F. D'Souza, *Chem. Eur. J.* 2013, **19**, 9629 and references cited therein.
- 45 S. K. Das, B. Song, A. Mahler, V. N. Nesterov, A. K. Wilson, O. Ito and F. D'Souza, *J. Phys. Chem. C* 2014, **118**, 3994.

50

## Table of Contents Graphic



5

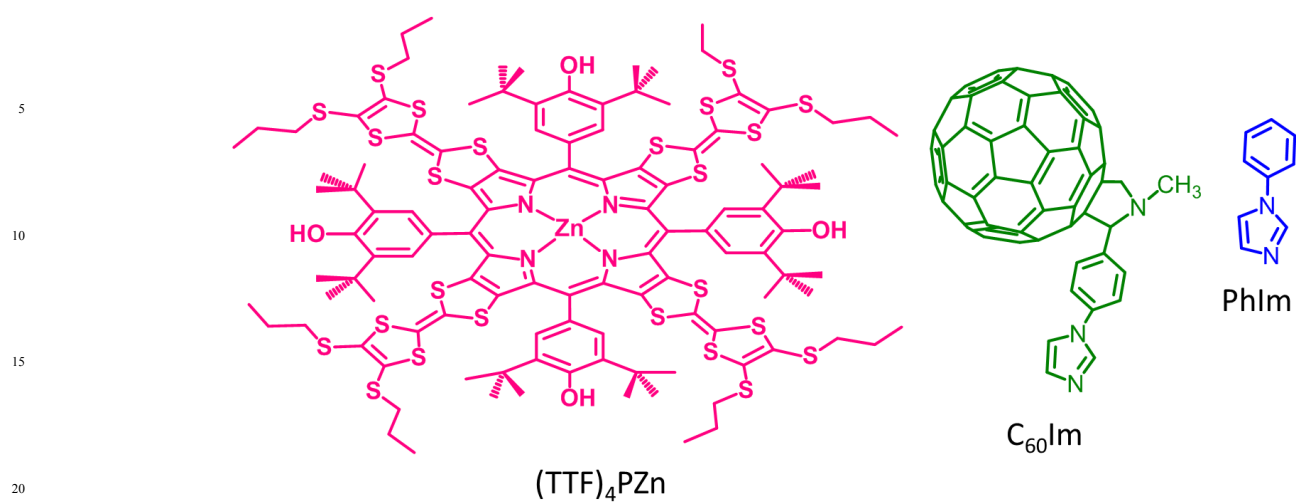
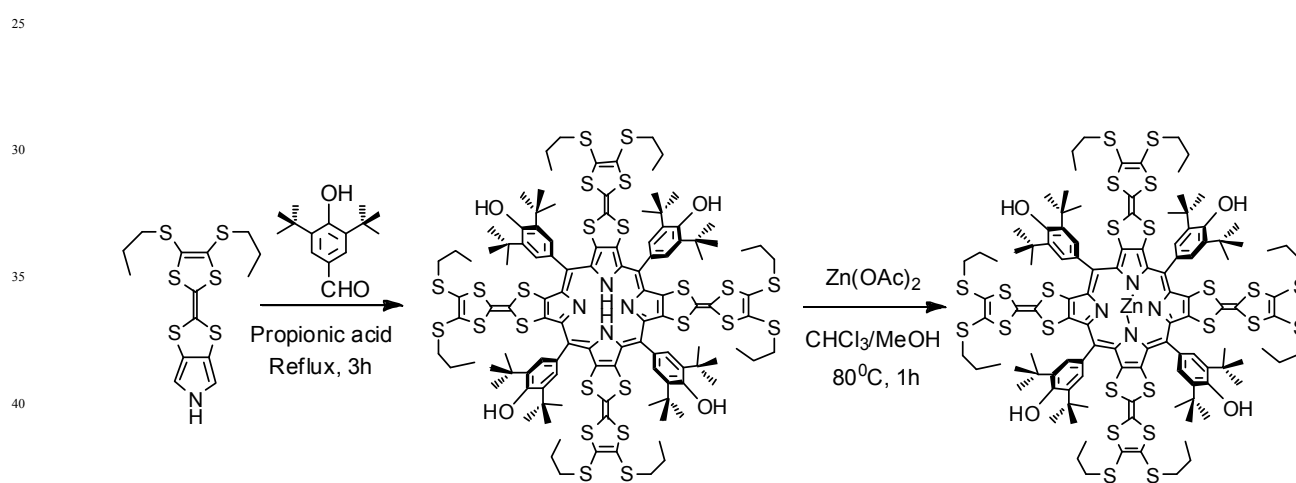


Fig. 1



Scheme 1

50

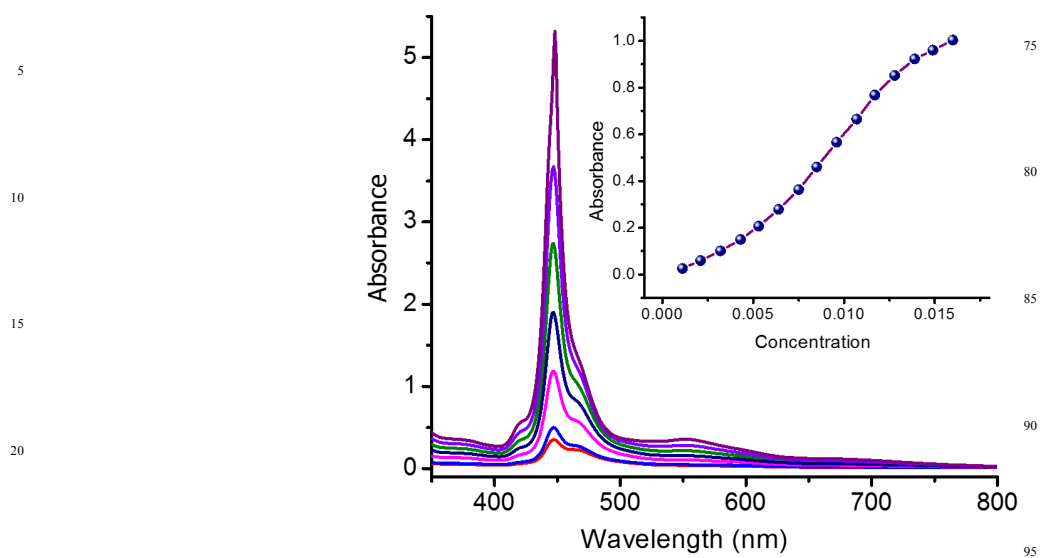


Fig.2

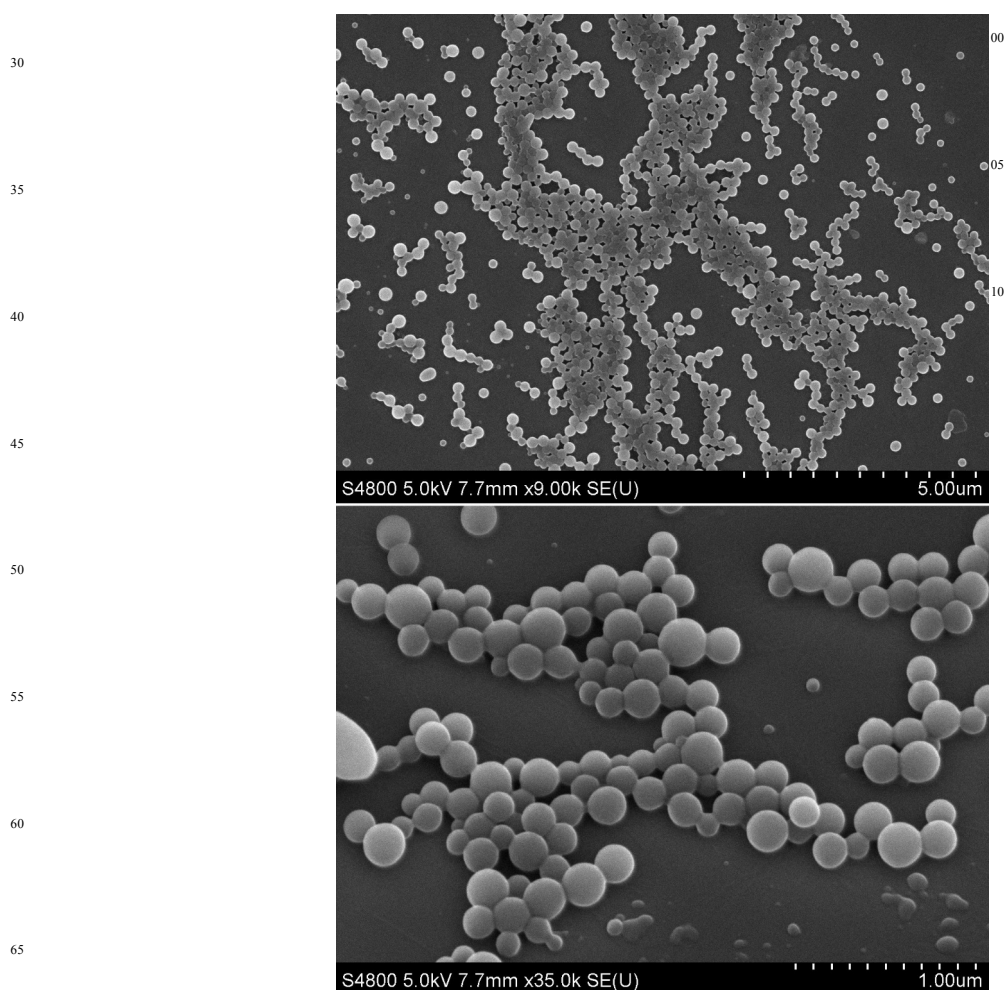


Fig. 3.

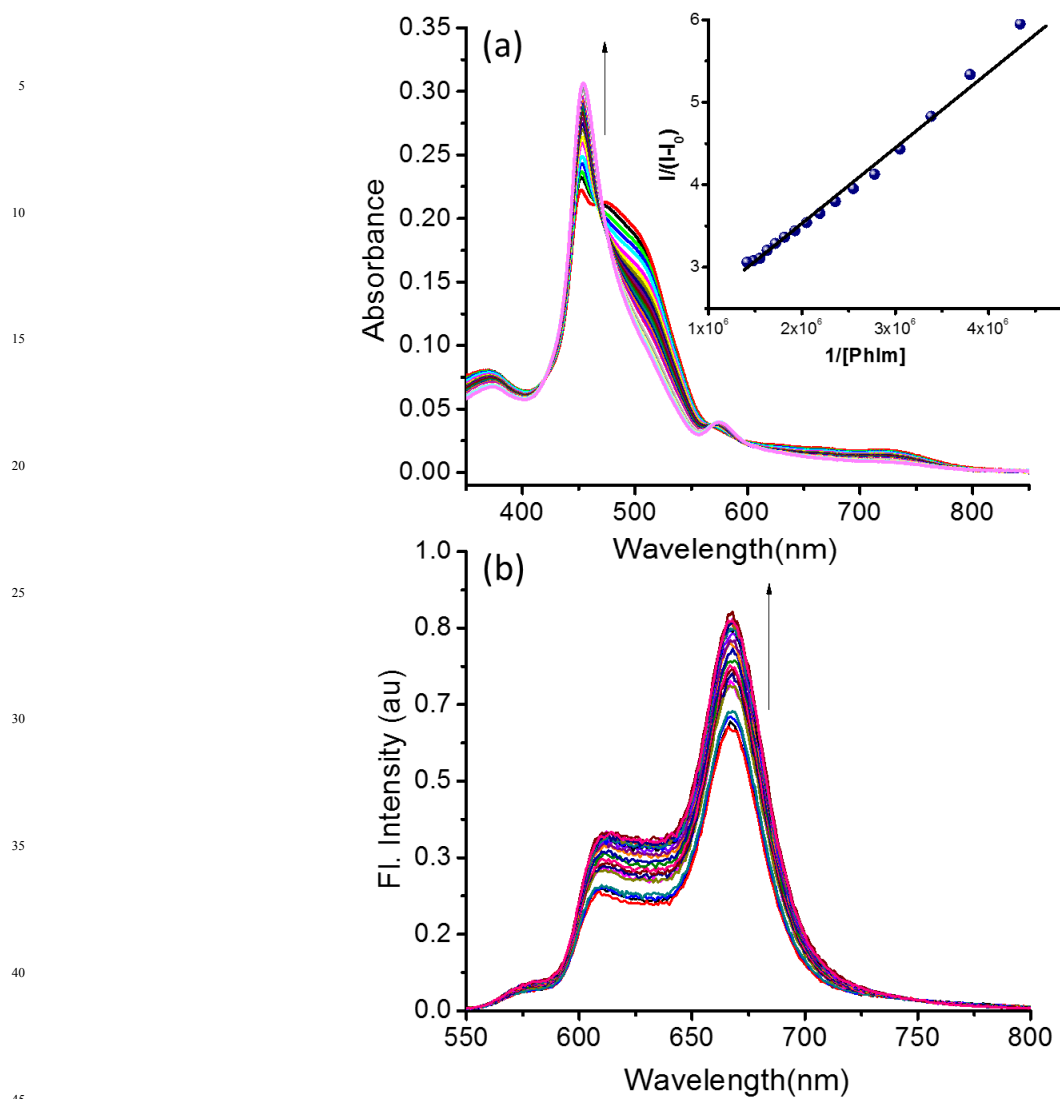


Fig. 4

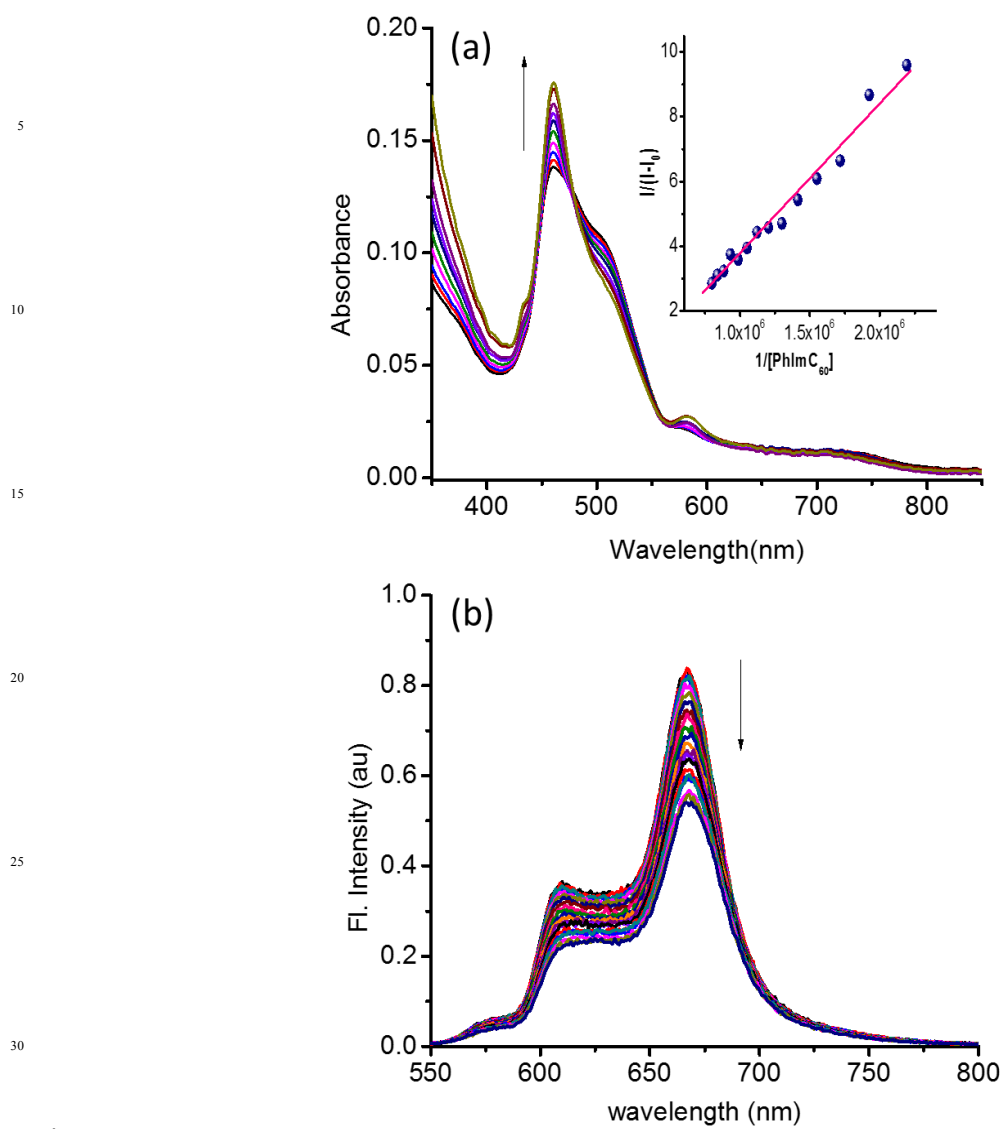
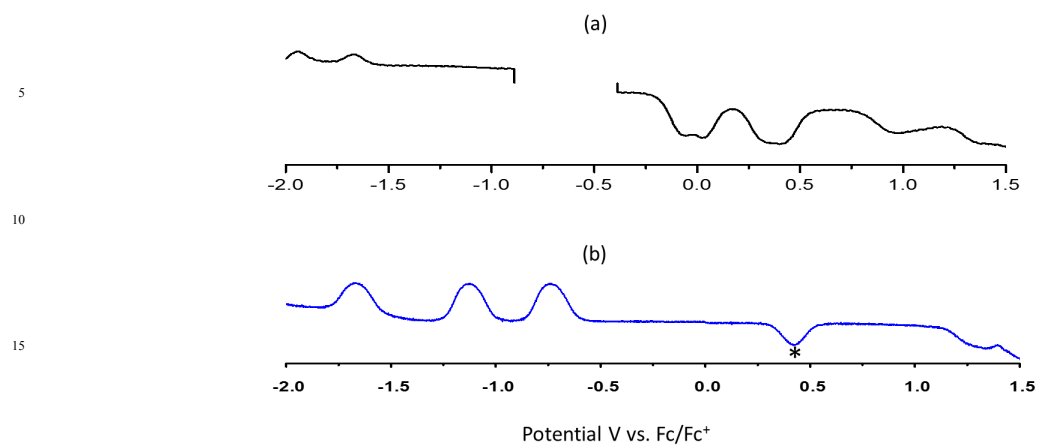
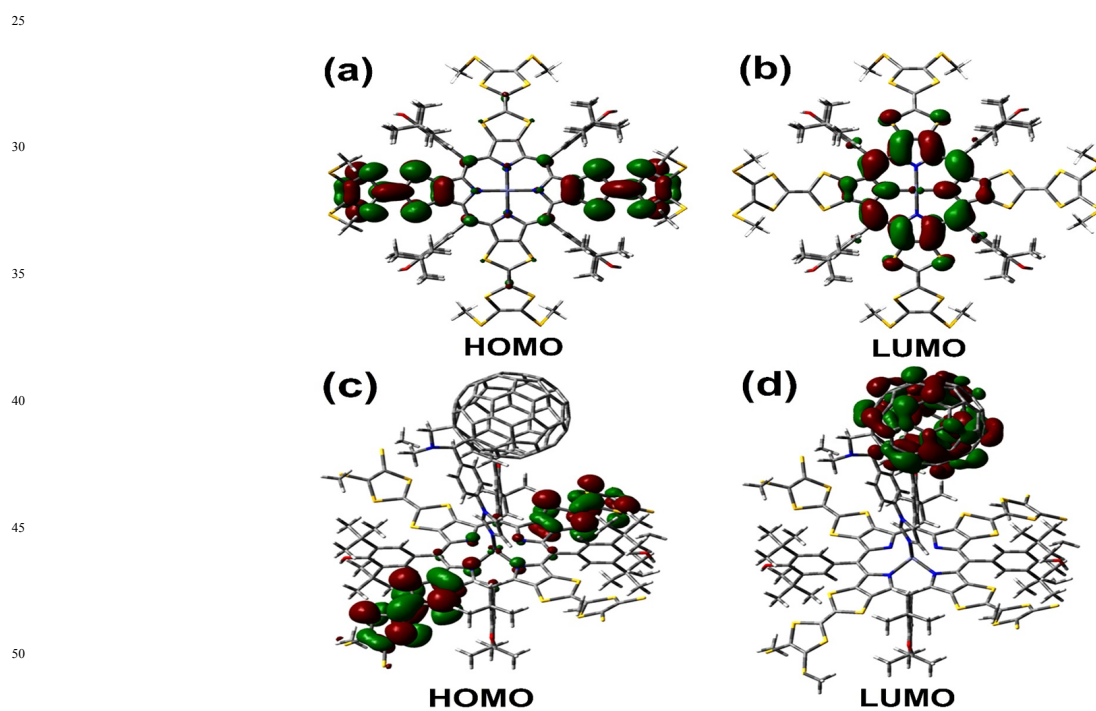


Fig. 5

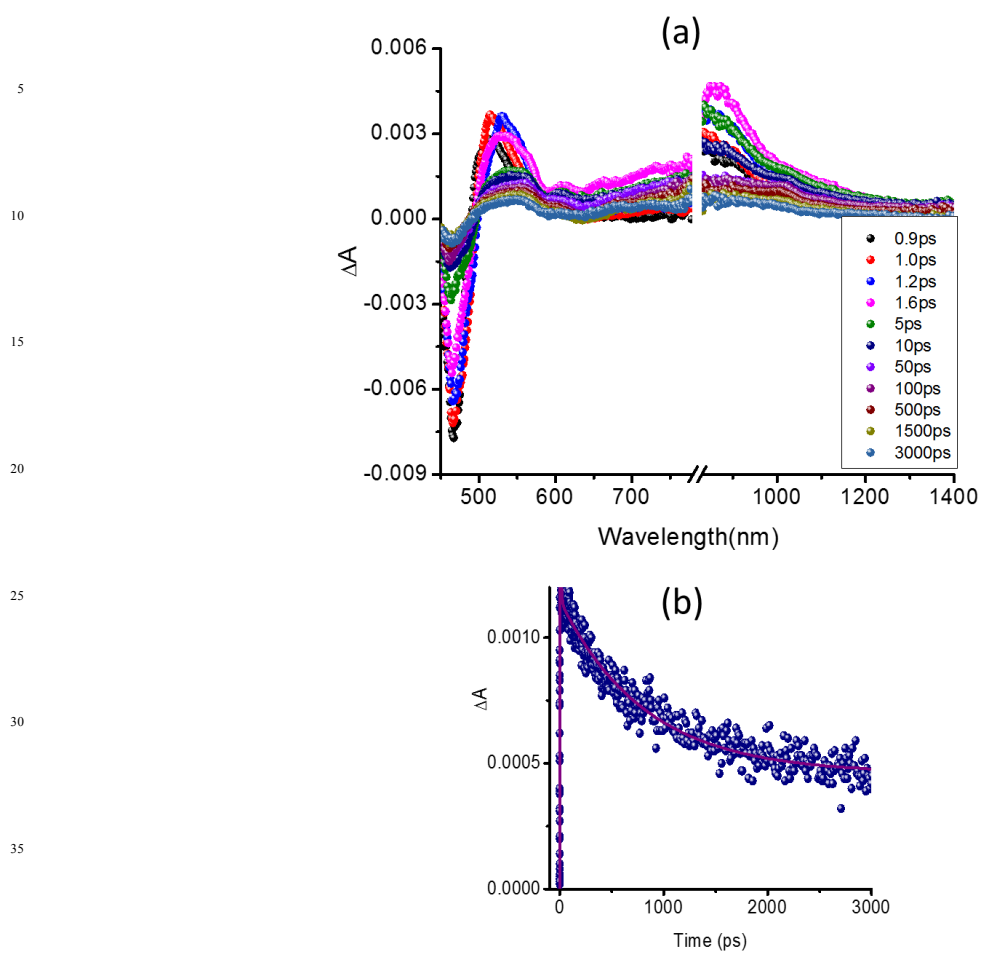


20 Fig. 6



55 Fig. 7

60



40 Fig. 8

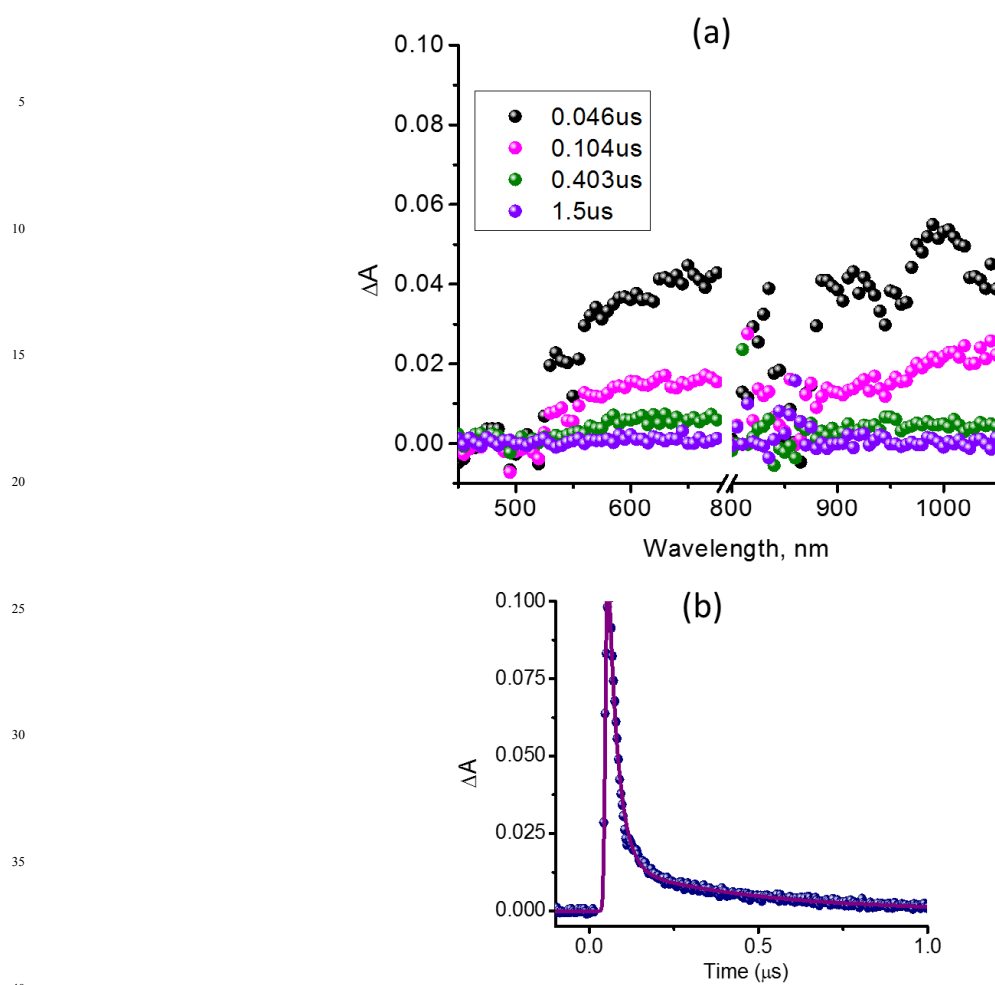


Fig. 9

